

5.5. Attitude Control Subsystem.

The IUE stabilization and attitude control subsystem consists of all equipment used to maintain or change the direction at which the spacecraft is pointing. In order for spacecraft attitude to be controlled, there must be some sort of attitude sensors, some equipment capable of producing a change in the orientation of the spacecraft (actuators) and an interface between the two. The IUE is capable of controlling attitude using a number of combinations of sensors, actuators, and interface.

This subsystem is without question the most complex subsystem aboard the IUE spacecraft. It was designed to be simple, light weight, low powered and reliable on one hand, and on the other hand, it was required that the control subsystem satisfy precise pointing and slew accuracy specifications. The principal requirements that have largely influenced the control subsystem design philosophy are the following:

- ▶ Three-axis stabilization in inertial space with a ± 1 arc second pointing accuracy requirement in pitch and yaw, for periods typically of $\frac{1}{2}$ hour and more.
- ▶ Following a slew or a sequence of slew maneuvers, a new source target must be acquired to within the 8 arc-minute half-cone angle field of the telescope.
- ▶ The pointing accuracy requirement must be satisfied for extended periods of time even when stellar attitude measurements of sufficient accuracy and frequency are not available.
- ▶ The expected useful operating life was to be 3 or 5 years.
- ▶ The stabilization and control subsystem was to be autonomous from a safety standpoint even though the spacecraft would be in synchronous orbit and in nearly continuous contact with the ground.

The attitude sensors include Earth and Sun sensors for use in ground computer aided attitude determination, accelerometers for on-board nutation control as well as rate gyro sets, analog Sun sensors for initial spacecraft acquisition, and an Inertial Reference Assembly, fine Sun sensors, and fine error sensors (or star trackers) for use in inertial star acquisition and subsequent hold and slew operations.

Hardwired analog control algorithms were incorporated to perform nutation control and all spacecraft initial acquisition functions as well as to provide an emergency rate hold function. The on-board computer was programmed to duplicate all the hardwired algorithms in addition to its primary attitude control functions of star acquisition, hold and slew.

For actuators, the IUE uses any three of the four reaction wheels in the hold and slew operations, and the hydrazine propulsion system in emergency attitude control and station keeping maneuvers.

5.5.1. Inertial Reference Assembly.

The Inertial Reference Assembly is the prime attitude sensor of the IUE spacecraft. The IRA consists of six single-degree-of-freedom, hydrodynamic gas bearing, rate-integrating gyroscopes with pulse-rebalance electronics.

A gyroscope can be described as an instrument that uses a rapidly spinning mass to sense and respond to changes in the inertial orientation of its spin axis. The gas bearing effectively eliminates the gyro bearing failure mechanism and significantly reduces its output noise, while pulse rebalancing provides a much improved readout accuracy as compared to analog rebalancing techniques. The assembly provides redundant analog rate information proportioned to body axis rates and digital attitude change information referenced to each gyro input axis. Each gyro senses inputs in all three spacecraft axes, by virtue of being skewed to all axes, as shown by the projections of the input axes of the six gyros on the spacecraft pitch-yaw plane.

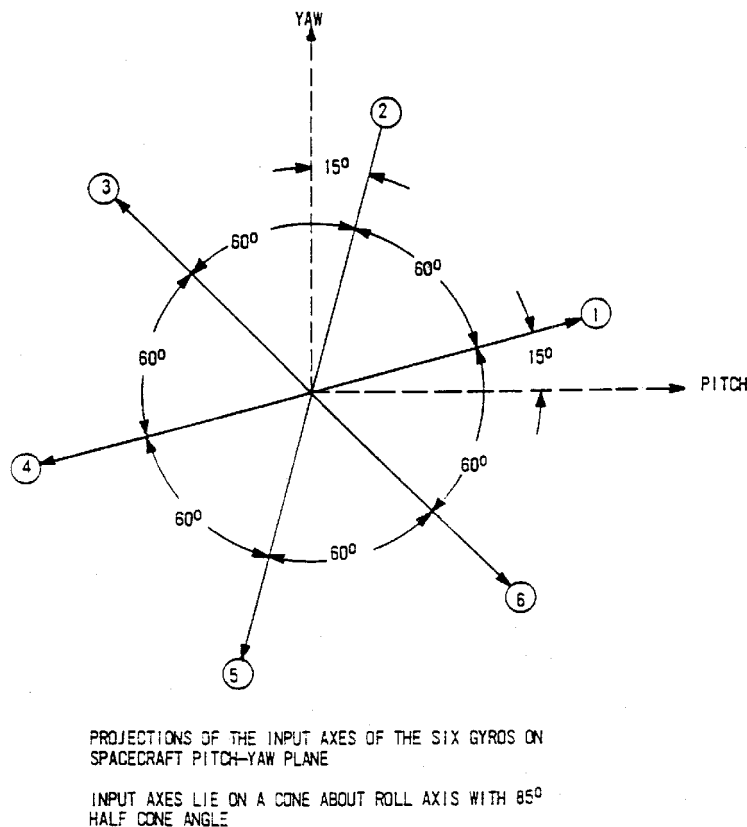


Figure 5-43. Projections of the input axes of the six gyros.

The OBC transforms and combines the gyro signals to create the composite control signals. Each gyro also generates analog signals to the control electronics assembly which drives the low-thrust engines and reaction wheels for analog Sun acquisition and Sun hold modes.

Each gyro has two operational modes and the resolution of each gyro is different in the two

modes. In hold/slew mode, the gyro generates digital signals with a resolution of 0.01 arcseconds. While in rate mode, the gyro generates analog signals with a resolution of 0.3 arcseconds.

The IRA was not used in the transfer orbit. Only the low-power heaters were on during this mission mode to maintain each gyro at or above 70° Fahrenheit. The following list summarizes the IRA modes used during the mission orbit:

- ▶ Despin. The IRA provided a redundant set of analog voltages proportional to sensed pitch, yaw and roll body rates. This information was used to automatically despin the vehicle from 5 rpm to near zero rates in all three axes.
- ▶ Respin. The IRA acted as a rate reference during the respin maneuver necessary for solar array deployment.
- ▶ Sun acquisition. Analog rate information from the IRA is mixed with position information from the course sun sensor to rotate the spacecraft. So that the sunline is normal to the solar array central panel and limit the rate of rotation about the sunline.
- ▶ Sun hold. Analog rate information from the IRA is mixed with position information from the course sun sensors to drive the pitch, yaw and roll reaction wheels and hold the solar array normal parallel to the sunline.
- ▶ Hold during velocity burn. Digital position information is provided by the IRA during this mission mode to permit the hydrazine system to operate without changing the spacecraft thrust axis inertial attitude.
- ▶ Backup sun acquisition and rate damping. Digital position information is provided by the IRA during those backup mission modes to permit an OBC algorithm to despin and stabilize the spacecraft in three axes.
- ▶ Hold/slew mode. Digital information is provided by the IRA during the mission to permit an OBC algorithm to hold the spacecraft inertial attitude in three axes and to slew the spacecraft from target star-to-target star.

5.5.1.1. Gyro failures.

At the end of the IUE spacecraft life, only the gyro 4 remained operational. The other five gyros were lost as is summarized below.

- **Gyro 6.**
During the first two shadow seasons, the 80% depth of discharge limit had been nearly reached on one battery, so it was decided to reduce the power load during the third shadow season by transferring operations to 3 gyros and turning off gyros 2, 4 and 6. On April 18, 1979, gyro 6 failed to restart.

The test carried out in an attempt to identify the gyro 6 problem indicated that the proper

amount of current was being drawn by the gyro. The gyro rotor was apparently stuck. All engineering procedures executed in attempting to restart gyro 6 were unsuccessful.

- **Gyro 1.**

Since June 28, 1981, the gyro 1 temperature had been slowly dropping. The drift rate was also changing slightly, which indicated that the change in temperature was real and not the result of a faulty telemetry thermistor.

On March 2, 1982 the gyro 1 was considered lost when its analog and digital telemetry was very quickly saturated, making it useless for either digital or analog control. The problem was diagnosed as a failure in the Pulsed Rebalance Loop of gyro 1's electronics.

In that gyro 1 had previously been judged unsuitable for use in the OBC's hold/slew algorithm, and was not in the gyro matrix used for attitude control at the time, the failure did not immediately impact operations.

- **Gyro 2.**

On July 27, 1982 the gyro 2 failed. Its motor current rose from a nominal 60 mA to 220 mA in 9 seconds. A similar problem had been observed in this gyro on August 18, 1981; the gyro current increased from 64 mA to 118 mA and then it returned to normal when the gyro was turned off and back on immediately.

In this failure, several attempts were made to start up the gyro by commanding it off then on again very quickly. This method did not work and so the gyro was turned off due to high temperature, the gyro 2 temperature increased to 69.3° C.

It appeared that the failure could be the result of a small particle jamming the rotor. During the turn-on attempts, maximum current was used to try to spin-up the gyro however no change in spacecraft momentum was observed.

- **Gyro 3.**

On August 17, 1985 the gyro 3 failed. Its motor current dropped from a nominal 60 mA to 2 mA and the spacecraft momentum changed quickly.

The spacecraft was put in sun-hold mode and the 2 Gyros/FSS backup control mode was loaded and enabled in the on-board computer. The commissioning of this system was successfully carried and on September 30, 1985 the observing program was restarted.

- **Gyro 5.**

On February 5, 1991, the gyro 5 motor current dropped from a nominal 60 mA to 0 mA and remained there. However, the gyro 5 continued to work properly and no change in spacecraft angular momentum was observed (the rotor continued to spin). The final manufactures conclusion was that gyro 5 prime winding was open, so its performance should be nominal unless it became necessary to restart gyro 5.

On March 6, 1996 the gyro 5 was switched off by a command conflict being sent to the

spacecraft and it could not be restarted. The IUE was placed in sun-hold mode and the previously prepared and tested One-Gyro control mode was loaded into the on-board computer. On April 4, 1996 the observing program was restarted.

5.5.1.2. Gyro Drift Rates.

Changes in the drift rates of the individual gyros caused some degradation of the spacecraft maneuvers and had to be corrected by updating the gyro scale factors in the OBC. New scale factors were calculated using data from maneuvers. The scale factors only changed rarely, and only once after 2 Gyro/FSS system implemented.

During the last years of the mission, the gyro 5 drift rate increased very quickly, which was associated with the degradation of the gyro's condition. At the same time, gyro 5's drift rate was subjected to short term fluctuations, which were thermally induced. In order to correct all these variations, the gyro 5 drift rate offset was updated very frequently during normal operations.

The gyro counts were converted to differential angles following the equation below.

$$\text{ABD (differential body angle)} = \text{WG (scale factor)} * \text{Gyro counts} - \text{BGDT (drift rate offset)}$$

The figure 5-44 shows the gyro drift rates along the whole spacecraft life.

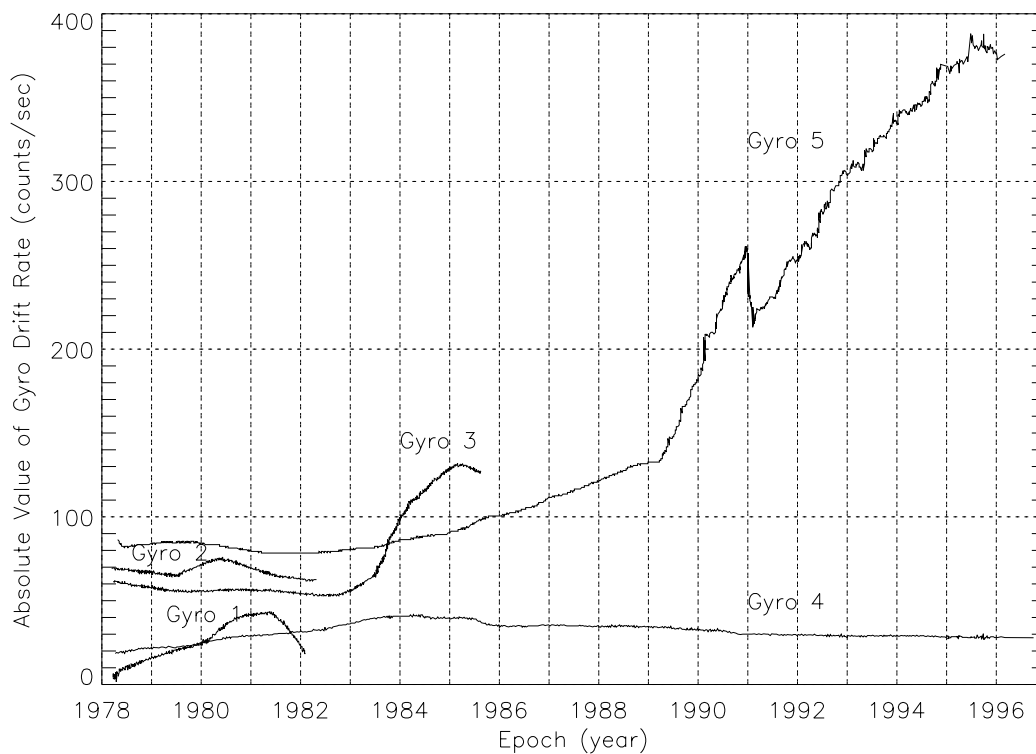


Figure 5-44. Gyro drift rates.

5.5.2. Fine Sun Sensor.

The Fine Sun Sensor (FSS) is a Digital Sun Sensor, which measures the spacecraft's position relative to the sun. In the pitch direction (rotation about the Y axis) the FSS measures the angle between the XZ component of the sun vector to the spacecraft -X axis, which is known as the beta angle (β). In the roll direction (rotation about the X axis), the FSS measures the angle between the YZ component of the sun vector and the +Z axis.

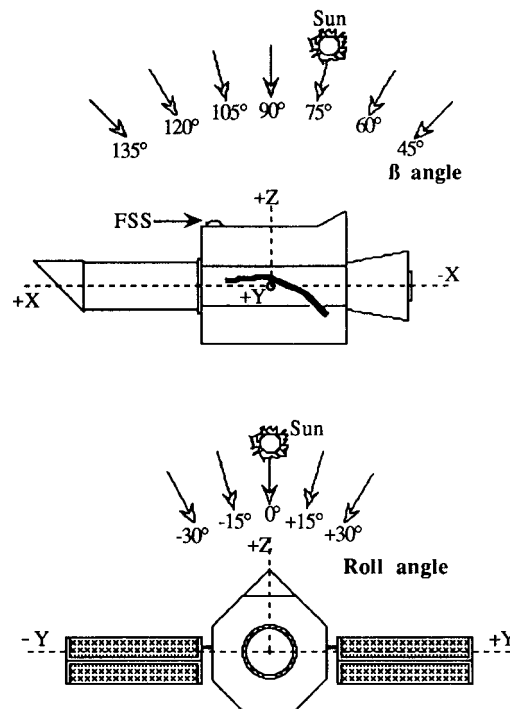


Figure 5-45. Definition of the beta and roll angles.

Two independent FSS systems are used to provide functional redundancy. Each system consists of two sensor heads and a separate electronics unit. The orientation of the two systems is identical. The heads are set up in such a way that Head 1 can view the sun from beta angles ranging from 137° to 73° and Head 2 can view the sun from beta 77° to 13° . Both heads are designed to sense the sun up to $\pm 32^\circ$ in Roll. In this way, sun presence could originally be maintained from beta 13° to 137° and at any Roll angle from $\pm 32^\circ$. During the IUE life, both systems were powered on and the following combinations were used during normal spacecraft operations; System 1/Head 2 for operations below beta 75° and System 2/Head 1 for operations above beta 75° .

Each sensor has two reticles, a fine reticle and a coarse reticle, for each axis. The course reticle encodes the Sun angle in six-bit Gray code format over the field of view to an average resolution of 1° . The fine reticle produces a quadrature sinusoidal output with an average period of 2° . The quadrature outputs are combined with four quadrature square waves to give a position signal whose phase angle is proportional to the Sun position within the 2° reticle period. This phase angle is measured by counting the number of high frequency reference pulses that occur between

zero crossings of the position signal and a reference ac signal.

The overlap between the 2° period of the fine reticles and the 1° resolution of the coarse reticles gives two digital values, NA and NB, which are transferred to the OBC and ground. These values are put through nine-term equations with the end result being a beta and roll measurement.

The FSS resolution is dependent of the actual sun to spacecraft angle. Both the beta and Roll angles affect the sensitivity of the FSS. The figure 5-46 and 5-47 show how the resolution varies with beta. Betadel is defined as the difference between the calculated beta angles corresponding to a FSS output measurement differing by a single count in the least significant bit weight position.

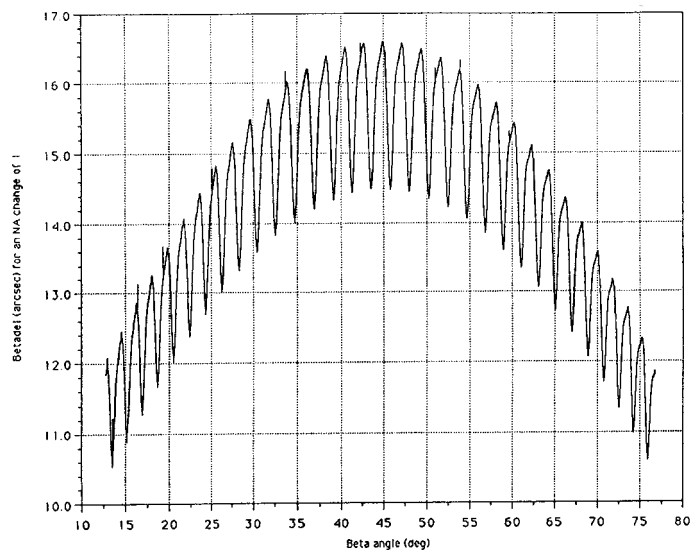


Figure 5-46. FSS beta and roll resolution vs beta angle.

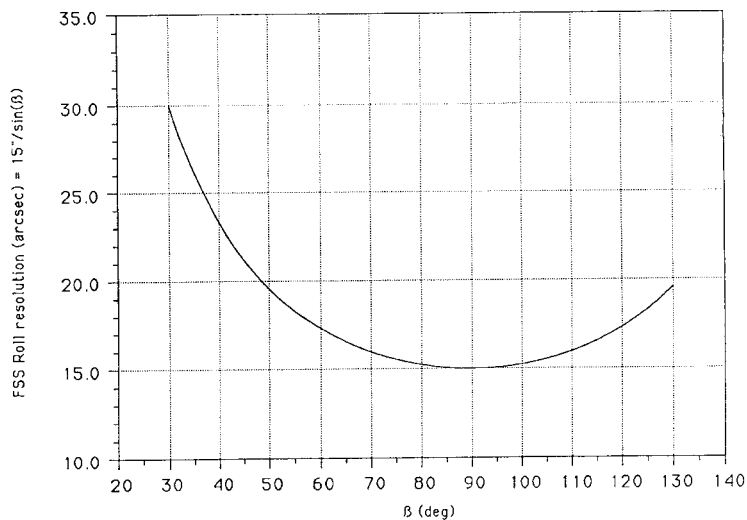


Figure 5-47. FSS beta and roll resolution vs beta angle.

While the FSS was always used as an attitude reference tool, its importance to the IUE mission was not fully realized until the middle of 1985, when the fourth of six gyros failed. This left IUE with 2 remaining gyros, FES, and the FSS to build an useable attitude control system. The 2-Gyros/FSS system used the FSS to control the Roll axis and, also, for position control on the Pitch axis during slews. After the fifth gyro failed, the 1 Gyro control system had to be implemented. In the default mode, when there was not any available star to guide on, the FSS data was used to control both the pitch and roll axis with position and rate information. The yaw axis was computed using gyro 4 information corrected with FSS data to remove Pitch and Roll components.

5.5.2.1. FSS anomalies.

Until April 1986, no reported spacecraft anomalies involved the FSS. It was noticed that in 1986, the ability of the FSS to correctly sense the sun position at beta angles less than 20° had degraded.

On March 9, 1988, it appeared that the degraded region slowly grew towards higher beta angles causing a loss of attitude control while the spacecraft was slewing at beta 22° . At the end of the maneuver the FSS gave corrupted data to the OBC in such a way that the maneuver continued towards lower beta angles and the sun presence was lost. The spacecraft had to be stabilized by commanding the sun hold mode. Shortly thereafter it was decided to limit spacecraft operations to beta angles above 28° .

On July 29, 1988 a spacecraft test was performed to determine the feasibility of switching to the redundant FSS heads. A switch would have been desirable if the redundant heads offered an improvement to the existing FSS operating limits. This proved to be useless. The back head (system 1/head 1) provided worse data than the prime one (system 2/head 1).

In 1990, a new corruption to the FSS data was observed. Because the sensor is not perfectly aligned with the spacecraft axes, the FSS roll angle not only has a component in the spacecraft roll axis, but also contributes a small amount to the spacecraft pitch angle, beta. In 1990 it was discovered that the information coming from the FSS roll axis had become corrupted and was adversely affecting control in both the pitch and roll axes. An investigation into this event showed that one of the 6 Course Gray code bits that come from the FSS roll axis was intermittently dropping out (from 1 to 0), and that it was happening consistently in the beta region between 35° and 38° . A software workaround was uplinked to the OBC to detect this situation and correct it.

While the spacecraft was controlled by the 2 Gyros/FSS system, the regions in which the FSS produces corrupted data had been increasing in number for several years, but had been compensated by restricting operational beta ranges or by implementing software patches. While an increase in anomalous functioning would be expected as the spacecraft aged, the lack of reported FSS anomalies prior to the implementation of the 2 Gyro/FSS system probably resulted from the use of this sensor in only a secondary manner. Anomalous FSS readings would not have been as noticeable since they would not impact the attitude control function.

On the 1 Gyro system, the effects of the FSS corrupted data have a more significant impact than they had on the 2 Gyro/FSS system. The yaw was now affected by corrupt FSS data as well as

the pitch and roll axes. The affect of corrupt FSS data on the yaw axes as well as an inconsistent handling of overflows by the onboard computer would typically cause a loss of spacecraft attitude under the 1 Gyro system.

5.5.3. Course Analog Sun Sensor.

The course analog sun sensor is used to provide two-axis attitude information with respect to the spacecraft pitch and roll solar array paddle axes. Six sensors (2 for roll, 4 for pitch) are utilized and are arranged to provide 4π steradian coverage. The output of the CSS is in the form of an error from roll equals 0° and beta equals 67.5° .

The CSS resolution is approximately 1° . So, the pitch and roll sets would both yield a sensor null when the Sun is at some point within 1° half-cone of the CSS null axis (roll equals 0° and beta equals 67.5°). The information from the CSS was used to drive the reaction wheels in the sun hold mode (Sunbath mode). Because the CSS did not have a yaw component, this axis was not controlled in the Sunbath mode, the spacecraft would spin about the yaw axes while the pitch and roll axes were maintained.

5.5.4. Spin Mode Sun Sensor.

This system consists of a single sensor head and its associated electronics package. The sensor field-of-view is $180^\circ \times 0.5^\circ$. Spacecraft alignment is such that its field-of-view is centred on -Z axis along the spacecraft X axis. This sensor also provides a sun centred pulse as the field-of-view sweeps past the sun.

The SMSS was used in the transfer ellipse to measure sun angle with respect to the spacecraft X axis.

5.5.5. Panoramic Attitude Sensor.

This system consists of two redundant sensor heads each having a dedicated electronics package. Each head provides a redundant 4π steradian coverage from a spinning spacecraft for earth/moon “look” angles and a sun-centred pulse so that “spin-sectoring” can be accomplished during the transfer ellipse.

The PAS was used during the transfer orbit and, in addition, was used to help establish spacecraft attitude prior to stellar acquisition.

5.5.5.1 PAS anomalies.

The PAS 1 failed shortly after launch. On January 29, 1978 the PAS counters continued displaying data present for 30 minutes after expected loss of signal had occurred. The failure

seemed to be a chip failure in the data register.

On April 30, 1985 both PAS's were turned off. The purpose of this action was to reduce the IUE power consumption and thereby increase the range of power positive beta angles. The PAS 2 had not been used for the last four years and, in case the spacecraft attitude was lost, there was other available recovery modes.

On August 28, 1985 a test was performed to see if the PAS 2 was still operational. It was turned on and a camera image taken. The stepping motor of the optical scanner would cause noise in the image if it was operating, but this test showed none. The PAS 2 was no longer working.

On July 29, 1988 an attempt to discharge the batteries was made. For this reason, both PAS's were commanded on, but only PAS 1 drew current. Analysis of the data suggested a relay failure for PAS 2.

5.5.6. Accelerometer.

This system consists of redundant, linear force-rebalanced accelerometers. The redundant accelerometers are aligned such that their input axes are parallel to the vehicle thrust (or spin) axes. Information from these units was used to implement active nutation control during the spin portion of the mission.

5.5.7. Fine Error Sensor.

The Fine Error Sensor (FES) is a photometer which performs the star tracker function on the IUE spacecraft. Because the FES is not internally redundant and because of its importance to the mission, two FES's are installed in the IUE. Near on-axis energy passes through one aperture of either two sets of aperture holes in the fold mirror at the telescope focal plane. One set of holes, the small apertures, are 3 arcseconds in diameter and the other set of holes, the large apertures, are ovals 10 arcseconds by 20 arcseconds. This plate also contains the fiducial lamps, which are used as references to determine star positions relative to the apertures, and a low reflectivity patch near the center that attenuates star images by five orders of magnitude. The FES's receive all of the off-axis energy, which is divided by a beam splitter in a 70/30 percent ratio. As a result, the FES receiving the 30 %, FES 1, is about 0.93 magnitude less sensitive, and the FES that receives the 70 % share is designated the prime unit, FES 2.

The FES operates in various modes, which are based on counting the number of photons of sufficient energy impinging on a 12.62 arcsecond square or pixel of photo-cathode surface and then electromagnetically shifting this square in discrete steps in various fashions. The total number of photon-events counted will be a function of stellar radiation within the square and the length of time that the count is continued. This digital count can be compared with commandable preset values to establish magnitude thresholds. If the stellar flux is excessive and/or the counting period is excessive, the counter will become inhibited at a count of 28,672 photon-events.

Basically, the FES uses this pixel in either of the two following deflection modes:

- The search deflection mode is a square raster formed by a repeated step and dwell sequence. The start coordinates and size of the square are commandable functions which make it possible to position the raster square anywhere in the tracker field and trade off raster scan time against raster field size.
- The track deflection mode consists of a four position, symmetrical pattern, centred about the sensor's latest determination of star position. Photo event data collected from opposite sides are compared and used to determine the relative position of the star image to the dwell points of the scan. In order to accommodate the wide dynamic range of star intensities, the dwell times at the four points of the track pattern can be selected between 0.048 seconds, fast track, and 0.192 second, slow track. The distance of the opposite points can also be selected between 10.8 arcseconds, overlap, or 31.3 arcseconds, underlap.

The FES combines these modes with logic operations and dwell periods to function in one or another of three system modes called primary, search and track, and field camera mode.

- Primary mode. In this mode track deflection is used to track a guide star in the FOV of the FES. The ground command specifies the approximate location of the star to be tracked, the track pattern size (overlap/underlap) and the track scan rate (slow/fast) to use. These combinations are capable of tracking guide stars from +14 magnitude to +2 magnitude. The accuracy achieved is approximately 0.27 arcseconds, which is considered as a fine unit (32 fine units are called a course unit).
- Search and track mode. This mode is used to automatically search out a particular magnitude star by forming a commanded square raster and proceeding to track the first star encountered which exceeds the commanded threshold. First, the search deflection mode is used and then, once the star magnitude threshold is exceeded, the FES switches to the track deflection mode and tracks the star.
- Field camera mode. This mode is used to map the star field within a commanded FOV. Search deflection, synchronized with the telemetry system, is used to accomplish this search. A signal from the DMU initiates readout of the sensor data and directly controls the stepping through the raster. So, the time needed to take the star field is directly proportional to the telemetry bit rate. The maximum field diameter is approximately 18 arcminutes, which corresponds to 4,063 fine units. The photon count data and position of each pixel is collected by the ground system and reconstructed into an image.

During the IUE life the FES has performed the following functions,

- ▶ The information from which initial IUE orientation in the celestial sphere was established was provided by the FES operating in the field camera mode. The ground computer used this information to recreate the telescope view. From this display, the astronomer performed comparison between the scientific instrument view and a star map until a pattern is recognized.
- ▶ After performing a slew, the FES operated in the field camera mode to recreate an image

on the ground. The astronomer identified the star field and designated one star in the pattern as the desired target star and a second one, when there was a second star available, as the guide star.

- ▶ After the slew is ended and the star field identified, the FES permitted manual or automatic acquisition of guidance stars. The search and track mode was commanded for automatic acquisition or the primary mode was used for manual acquisition. In any case, the FES was finally placed in the primary mode tracking on a star. In this mode, the FES generated a digital error signal showing the offset from star center to the commanded coordinates which was used to both center the track pattern on the star and provide an indication of off-null pointing.
- ▶ After the guide star was acquired, the FES provided two-axes error data from an offset star for either open-or-closed-loop positioning of the target star in the experiment aperture. The FES was also used to detect, quantize and correct the drift in the gyros. This was done by allowing the FES to track a guide star and then using the resultant errors either directly in the OBC algorithm or indirectly as ground computer generated gyro bias compensating for the drift.
- ▶ In the 1 Gyro control system, the FES was particularly important. The spacecraft used the FSS and the remaining Gyro to provide coarse control. So, the FES was necessary to accomplish fine pointing control. With the FES commanded to primary mode tracking on a guide star, the spacecraft could perform the small, very accurate slews needed to place the target in the desired aperture and start the exposure.

The figure 5-48 shows a null FES 2 image, which is represented in FES coordinates (X,Y). The relation between the FES axes (X,Y) and the spacecraft axes (P,Y) are also displayed. The fiducial lamps are named by letters.

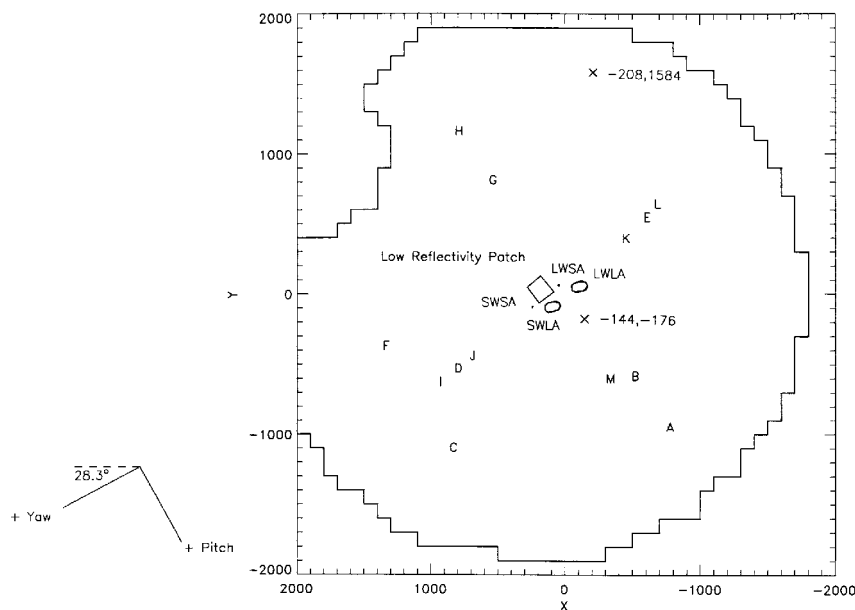


Figure 5-48. FES field-of-view.

The two x-marked points were known as the reference point (-144,-176) and the offset reference point (-208,-1584). During normal operations, the target was usually placed at one of them before it was moved into the aperture. In April, 1989 the first one (-144,-176) was chosen to replace the old one (-16, -208), which had lost sensitivity due to fatigue effects from repeated saturation. On March, 1993 the offset reference point had to be chosen in the less contaminated part of the FES field due to the FES streak light anomaly.

5.5.7.1. FES geometric calibration.

The FES suffers from geometrical distortion across its field of view. The overall pattern is that of a distorted S-shape. For instance, if a star is moved from one point to another in the FES field of view, the star will not be precisely at the expected point, but displaced by an amount roughly equal to the relative FES geometrical distortion between the star's original and final positions in the field. This effect had a great importance under the 1 Gyro control system, which had to rely on accurate positioning of a guide star in the FES field to place the target in the aperture.

Most of the distortion appears to come from the nature of the FES itself which is a magnetically focused device. In addition there appears to be an "edge effect". As one approaches the edge of the aperture plate, there is a general tendency for the level of distortion to rapidly increase, for the reflectivity of the aperture plate to drop, and the distortion to be radially directed away from the center of the FES. Data taking for the FES geometric distortion measurement indicated that the distortion was stable over the years.

The figure 5-49 shows the FES 2 distortion values.

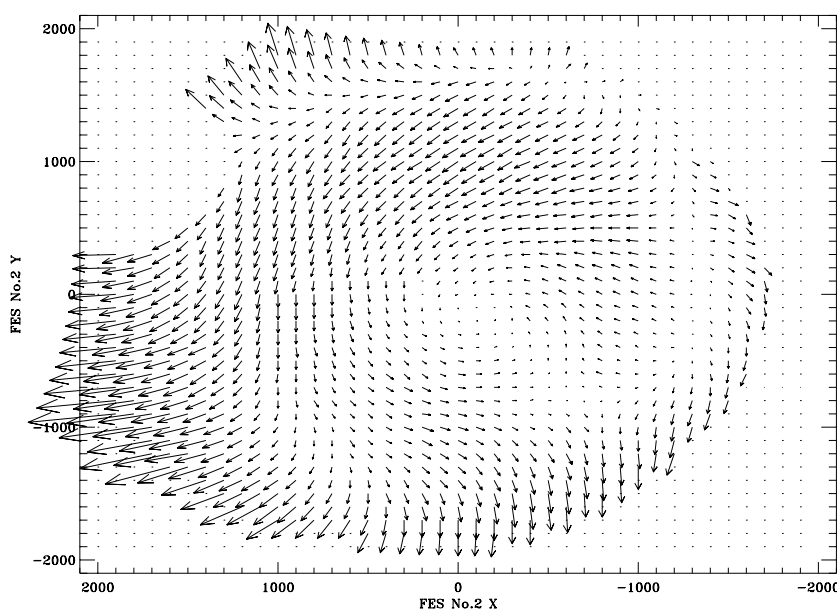


Figure 5-49. FES distortion values.

5.5.7.2. FES 2 reference point shift anomaly.

On October 25, 1979 an intermittent change of aperture locations in the FES 2 was noted. The usual drop of light did not take place when targets were moved into the small apertures.

A few months later, the same behaviour was seen again. The problem was thought to be related with the FES electronics.

On January 9, 1981 a test was conducted to analyze this FES problem. The result suggested that the apertures, the aperture plate, and the cameras are remaining fixed relative to each other.

5.5.7.3. FES 2 star count variations anomaly.

On April 15, 1985 an anomalous behaviour of the FES 2 was noted. During an observation of a star with known magnitude, count variations of up to 100 times of its known counts were seen.

Along the spacecraft life, several cases had shown similar behaviour. All cases occurred while having the FES configured in fast track/underlap mode and in a period when the spacecraft passed the radiation belts of the Earth.

5.5.7.4. Scattered light anomaly.

On January 27, 1991 an increase of background light in the FES was first noticed, which was called the scattered light anomaly. The following ideas were proposed as the cause of this problem.

- A FES temperature dependent problem.
- A hydrazine cloud reflecting sunlight. The hydrazine cloud could have been formed by the unloads performed on a routine basis.
- A Barium cloud with forward scattering of the 4554.03 resonance line of Ba II. On January 20, 1991 a barium canister was exploded at 30,000 km near the longitude of the IUE orbit.
- The sunlight could be coming in the telescope tube due to a pinhole caused by a micrometeoroid. Another idea was that insulation had been torn loose and was drifting on the opposite side of the tube-end from the sunshade.

Several tests were done in order to determine the cause of the light and its dependence on certain parameters (telescope tube temperature, beta angle, roll angle, etc). The following characteristics of the scattered light were determined:

- ▶ The scattered light was independent of the electronic configuration of the spacecraft. For instance, it was independent of the telemetry bit rate.

- ▶ The scattered light was present in both FES's.
- ▶ The scattered light was distributed in a uniform pattern over the FES FOV.
- ▶ The light could be made to disappear by closing the sun shutter.
- ▶ The spectrograph images were not affected by the scattered light.
- ▶ The light usually increased in intensity with increasing beta angle, as is shown in the figure 5-50.
- ▶ The light intensity decreased with positive roll angle.
- ▶ The FES scattered light is strongly affected by shadow season periods. The figure 5-51 shows the evolution with time of the FES background of two stars at beta 90°. Since the anomaly first appeared, the background became enhanced during each of the shadow seasons, but returned to pre-shadow levels after the shadow season was over. The exception to this is shadow season 30; the lack of an increase in the counts during the shadow season was thought to be the result of the deliberate attempts to pass shadow each day at beta angles less than or equals to 65°, thus minimizing the thermal shock experienced by the end of the telescope tube.

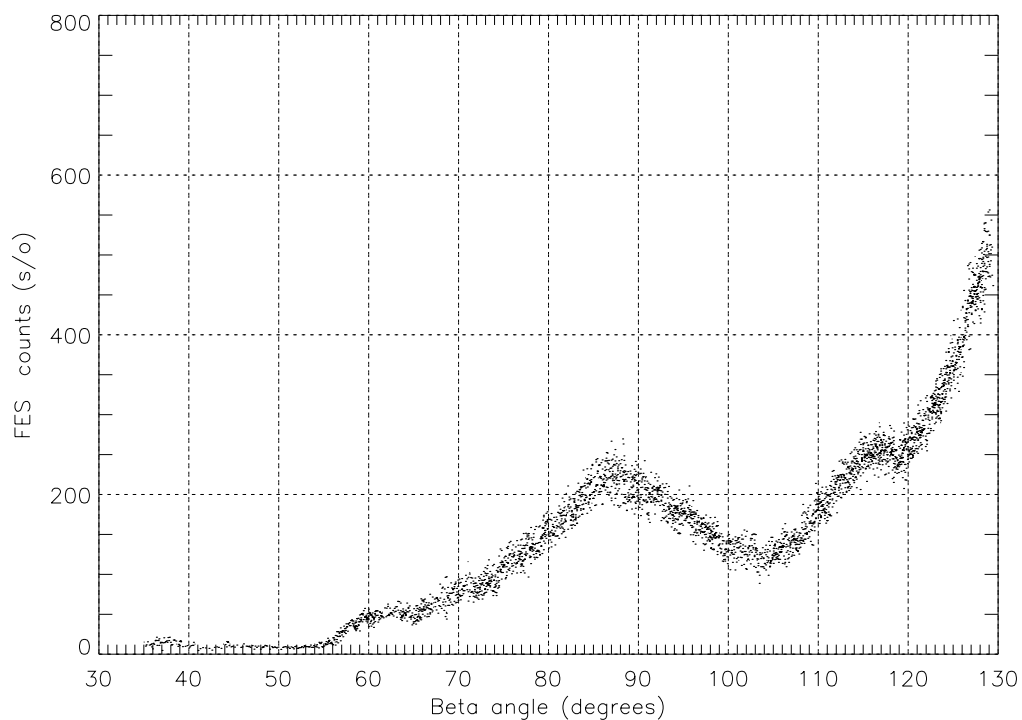


Figure 5-50. FES background counts (s/o) vs Beta angle on June 29, 1992.

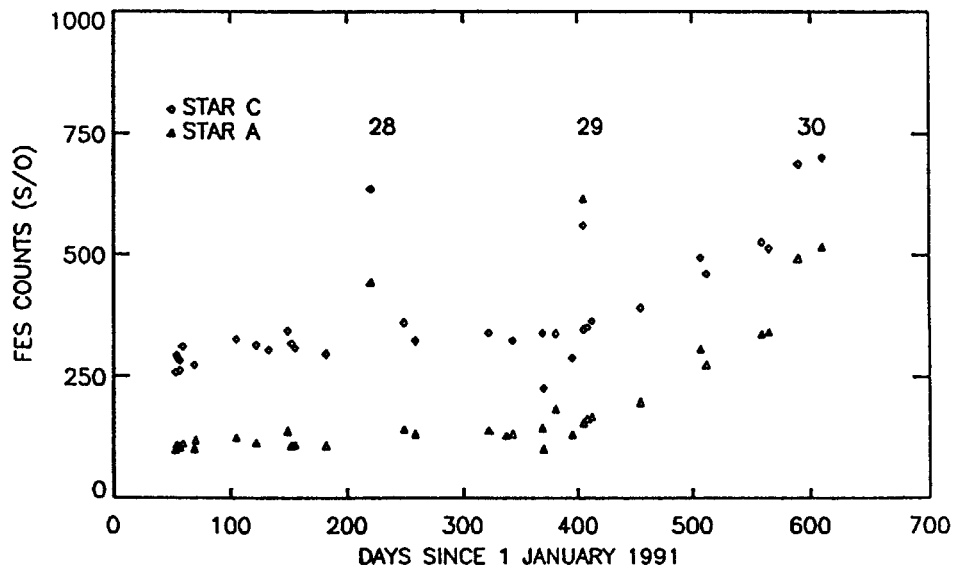


Figure 5-51. FES counts (s/o) vs since January 1991 until September 1992.

A 12.0 magnitude star is approximately equivalent to 225 FES counts slow track/overlap, and 11.0 magnitude, to 560 counts slow track/overlap. Fast track mode measures approximately four times less counts than slow track mode since its dwell time is one fourth the duration of slow track.

5.5.7.5. Streak light anomaly.

A significant enhancement of the scattered light was detected on September 14, 1992. This was known as the FES streak light anomaly and was mainly associated with Sun and Earth irradiation.

The behaviour of this anomaly was different than the previous light in several aspects.

- ▶ The light decreases with negative roll angles.
- ▶ The long duration long wavelength spectra could be contaminated.
- ▶ The light was always seen in the same area of the FES fields. A typical FES contaminated image is shown in the figure 5-52.
- ▶ The streak was highly variable. The figures 5-53 and 5-54 show the background measured during two similar maneuvers, from low beta to high beta and from a high beta to low beta respectively. So, one could attempt to reduce the extent of the streak in the FES by performing a straight pitch maneuver to beta 105°, then maneuver back at beta 90°. During the first year of this anomaly, this procedure dramatically reduced the level of the streak at beta 90°. The figure 55 shows the streak evolution during the last four years of IUE's mission.

The streak presented some difficulties for operations in the identification of the target field. It also precluded tracking on any guide stars which fall in the affected portion of the FES, unless they were high enough in magnitude to sit well above the level of the streak.

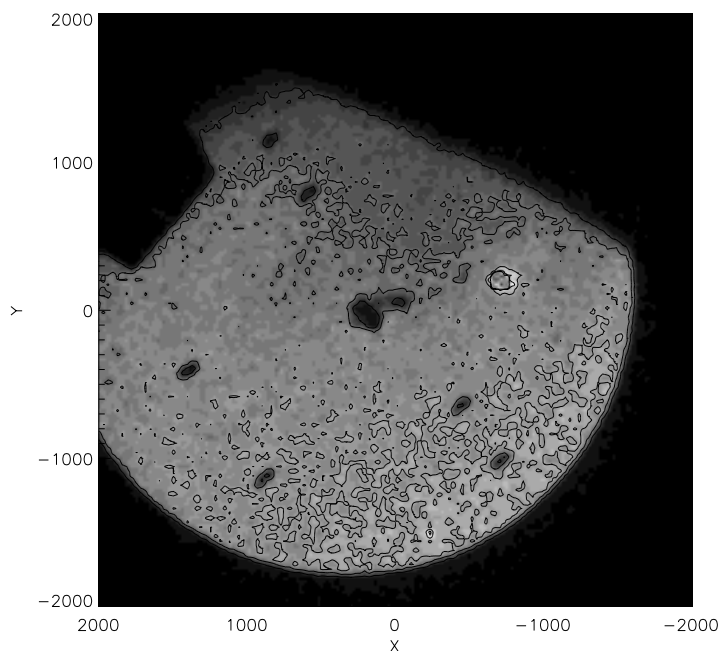


Figure 5-52. FES contaminated image.

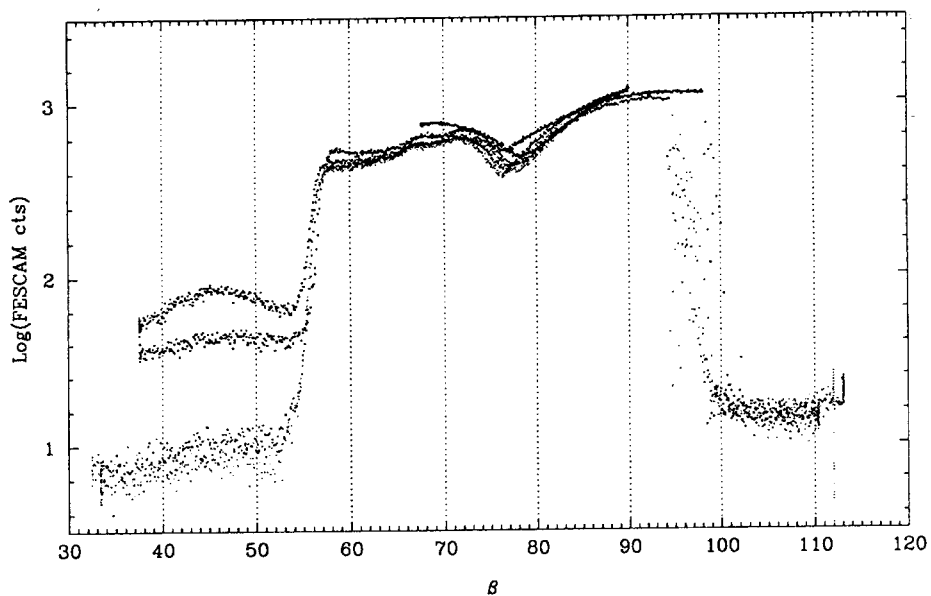


Figure 5-53. FESCAM counts vs β summarized maneuvering from beta 35° to 115° .

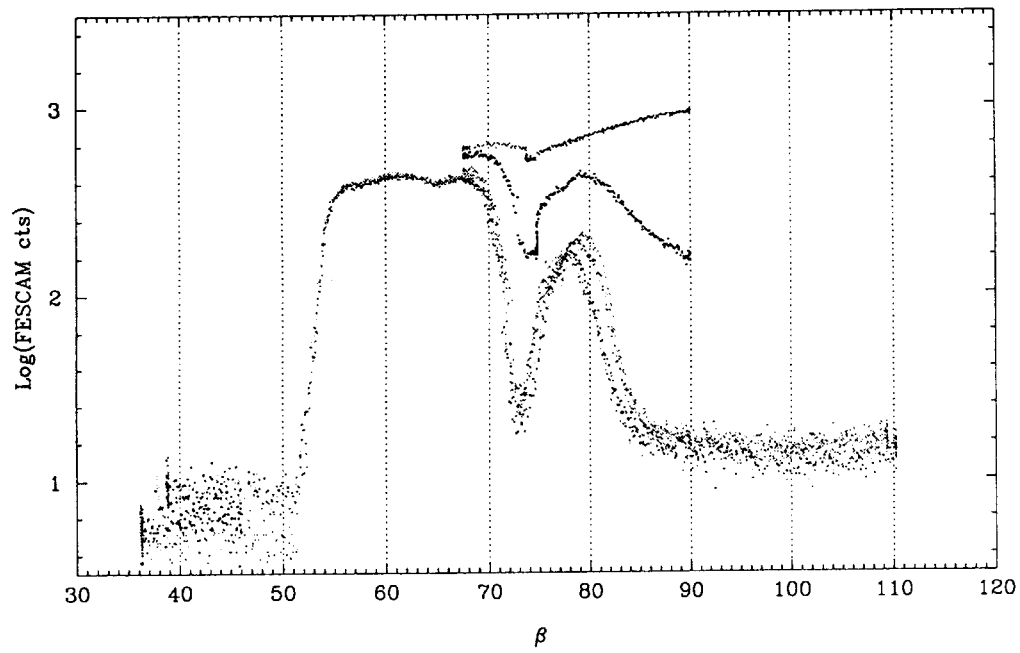


Figure 5-54. FESCAM counts vs β summarized maneuvering from beta 115° to 35° .

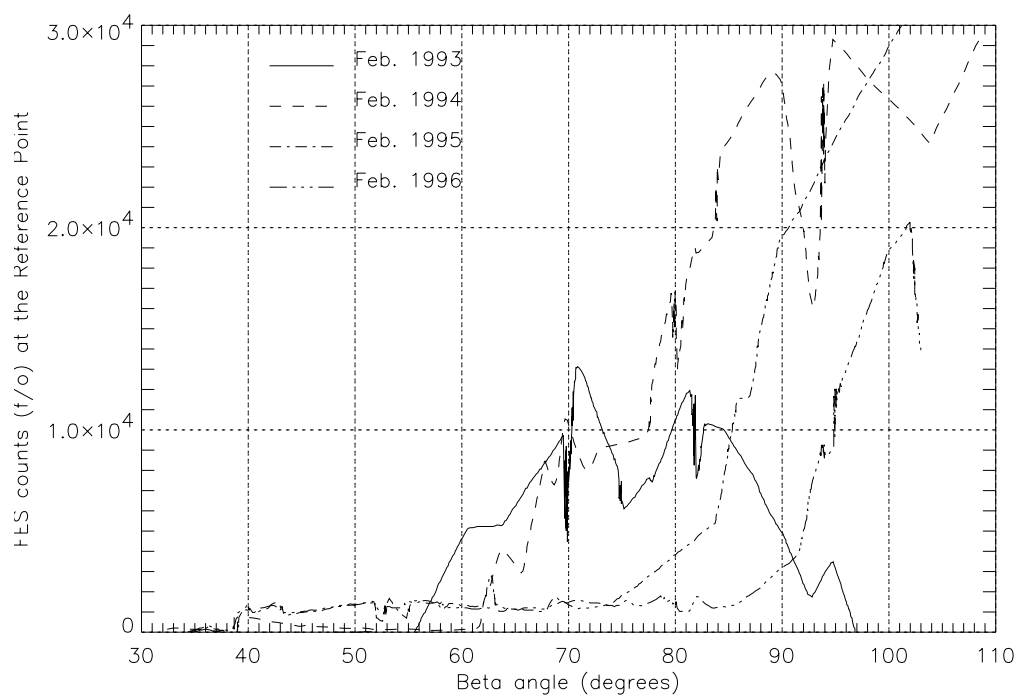


Figure 5-55. FES counts (f/o) at the Reference Point.

5.5.8. Reaction wheel.

The reaction wheel assembly consists of four wheels, four wheel driver modules and a redundant power converter. Three reaction wheels are aligned to the spacecraft pitch, yaw and roll control axes. The fourth wheel is skewed symmetrically with respect to the orthogonal control axes. This unique configuration provides redundancy in the event the pitch, yaw or roll wheel fails. During the whole IUE mission, the three prime wheels worked properly, so the redundant wheel was not used.

A reaction wheel is a rotating disk used to store momentum or transfer momentum to the spacecraft body for the purpose of executing slews. When the wheel is accelerated or decelerated, the reaction torque can be used as the actuating torque for an attitude control system. Thus, a transfer of angular momentum between the vehicle and the wheels is possible. The reaction wheels provide the following advantages for a three axis stabilized platform.

- ▶ The capability of continuous high accuracy pointing control.
- ▶ Large angle slewing maneuvers without fuel consumption.
- ▶ Sun hold acquisition.

The angular momentum that can be stored in the wheels is limited, so a secondary control system is used to prevent the stored momentum from becoming too high or too low. The secondary dumping system is a jet thruster system (HAPS). The reaction wheels must be kept within certain rpm limits to assure optimum control and to prevent bearing wear. The limits are as follows: Pitch ($|200|$ - $|1000|$ rpm), Yaw ($|200|$ - $|500|$ rpm) and Roll ($|200|$ - $|500|$ rpm). The momentum dumping operations are carried out during specified limited periods of spacecraft activities, so that unacceptable attitude errors are not introduced into the scientific instrument experiments.

Each wheel driver module generates a two phase square wave signal to drive its associated reaction wheel. Either half of the redundant digital to analog converter (DAC) and command decoder module provides wheel command information to the wheel driver module. The pitch, yaw and roll reaction wheel driver modules are also able to receive information from the compensation and mixing card (C&M) of the control electronics assembly (CEA). This card provides processed analog sun sensor information and rate information for the reaction wheels for use in the sun hold emergency mode.

5.5.9. Hydrazine Auxiliary Propulsion System.

The IUE hydrazine auxiliary propulsion system (HAPS) is a monopropellant catalytic hydrazine blow down propulsion system. It consists of six propellant tanks, fill/vent valves for each tank, fill/drain valves for each pair of tanks, pressure sensors, filters, seven latching valves, heaters, temperature sensors, twelve monopropellant engines (eight 0.2 pound low-thrust engines, LTE's, and four 5 pound high-thrust engines, HTE's) and an electrical junction box which contains all necessary connections, circuits and current shunts for the heaters and valves.

The HAPS unit comprises two physically distinct sections. The first section is located in the body of the spacecraft between the main equipment platform and the apogee boost motor, and contains the hydrazine fuel tanks, four LTE's and the associated lines and valves. The second section consists of two remote engine modules (REM's), which extend about 2 feet below the propulsion bay. Each REM contains two LTE's, two HTE's and the associated lines and valves.

The figure 5-56 shows a diagram of the HAPS assembly.

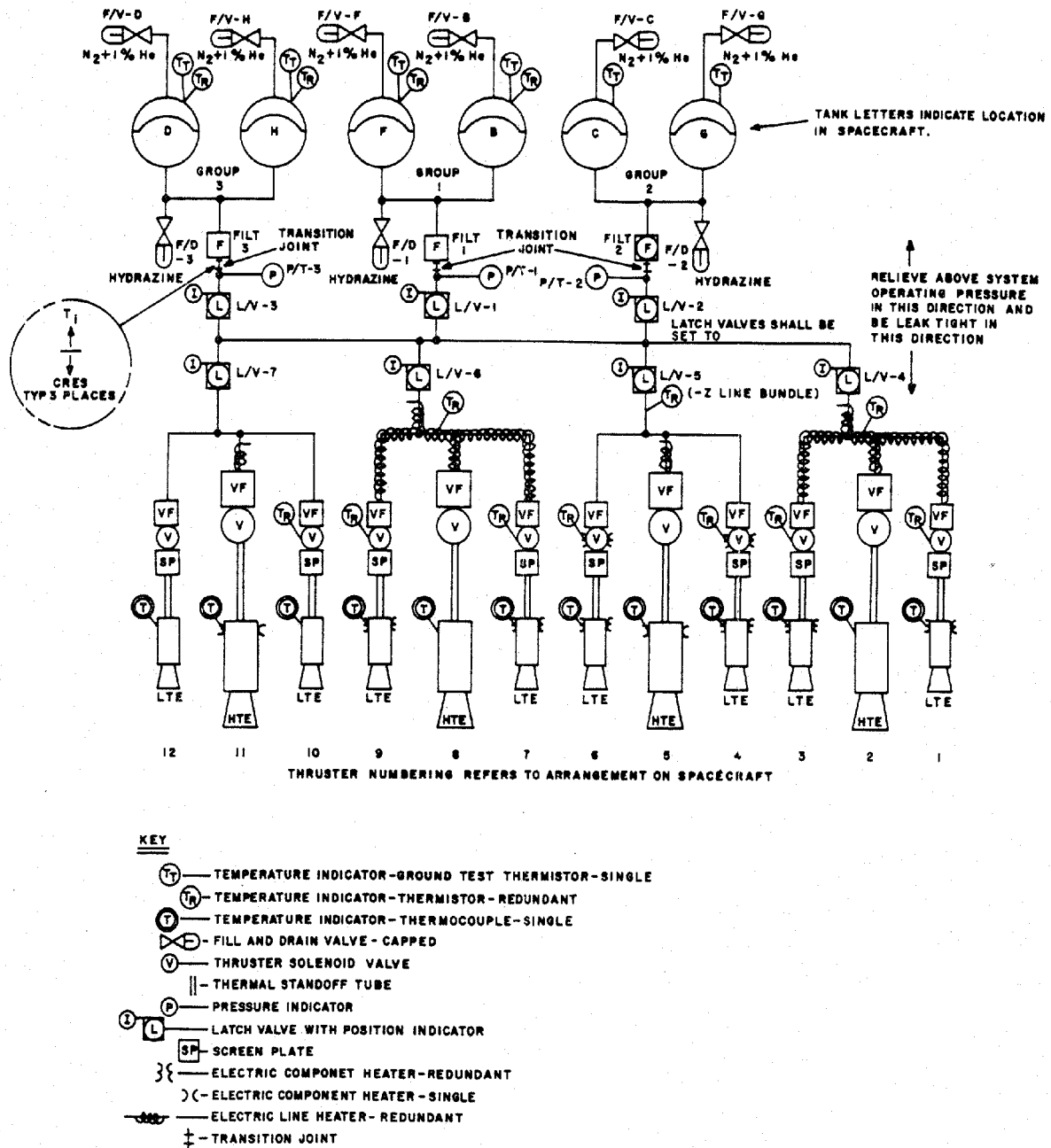


Figure 5-56. HAPS, schematic.

The tanks are connected in pairs and are located at equal distances from the spacecraft x axis. This arrangement permits fuel to be depleted from two, four or six tanks at once and permits system balance to be maintained. Each tank contains a flexible diaphragm to separate the hydrazine from the pressurizing gas, nitrogen. The hydrazine flows from the tank pairs through a common filter past a pressure monitor. A latching valve separates each tank pair from a common manifold which feeds four engine groups. Each group is separated from the rest of the system by a latching valve, which allows operations to continue if there is a component failure. The problem area is isolated from the system by closing the specific latching valve, and the secondary jet or tanks would be used.

The propellant, hydrazine (N_2H_4), was chosen for the IUE because it is fairly inexpensive, is flight proven, can handle both long and short jet firings, and will not contaminate the scientific instruments.

The system was originally loaded with 27.3 kg of hydrazine divided equally among the six tanks. Before launch, the system was filled with hydrazine down to the engine valves. All latch valves were closed and two tanks were pressurized to 200 psi, and the other four were pressurized to 350 psi. Once in orbit, latch valves 2, 4, 5, 6 and 7 were opened. Then, latch valve 2 was closed, and latch valves 1 and 3 were opened. This loading procedure was followed to prevent possible latch valve problems because of sudden pressure changes when the latch valves were initially opened. During the whole mission, the IUE had all latch valves open except latch valve 2. This valve separates the two tanks C & G, which were only used to pressurize the system initially following launch. The tanks could have been opened if needed but the other four tanks supplied sufficient N_2H_4 through out the mission.

The figures 5-57 and 5-58 show the temperature and pressure evolution in the tanks.

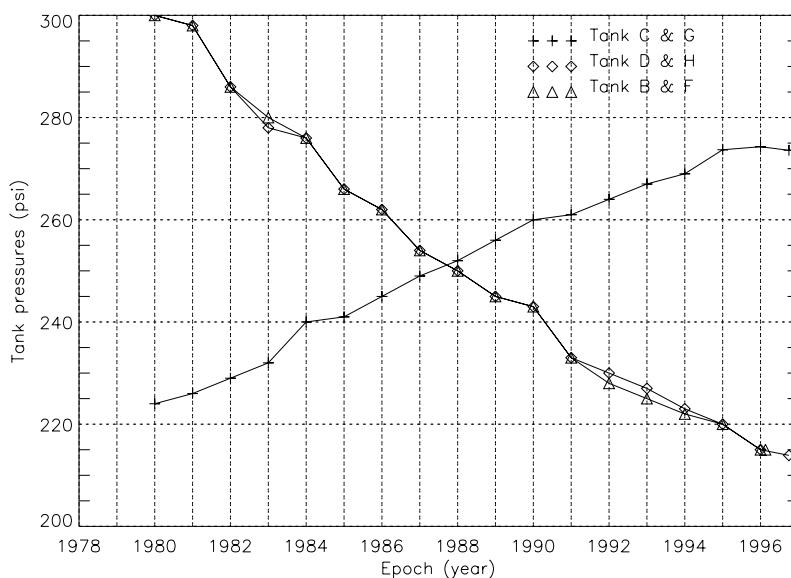


Figure 5-57. Tank group pressures.

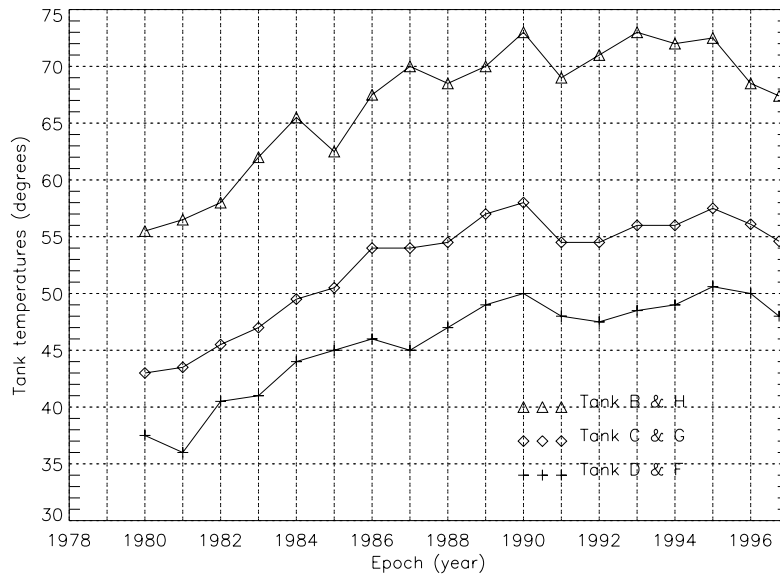


Figure 5-58. Tank group temperatures.

On February 18, 1996 the B&F tank pressure indication dropped to 14.2 psi, which corresponds to a raw telemetry value of zero for the tank pressure signal, and remained there. As, there was not any spacecraft momentum change, the failure was assigned to the pressure sensor for Tanks B&F, either directly or in the wire connections to the telemetry system.

Prior to the N_2H_4 venting on September 30, 1996 there was approximately 17.7 kg of hydrazine remaining in the tanks. The figure 5-59 shows the hydrazine consumption during the mission.

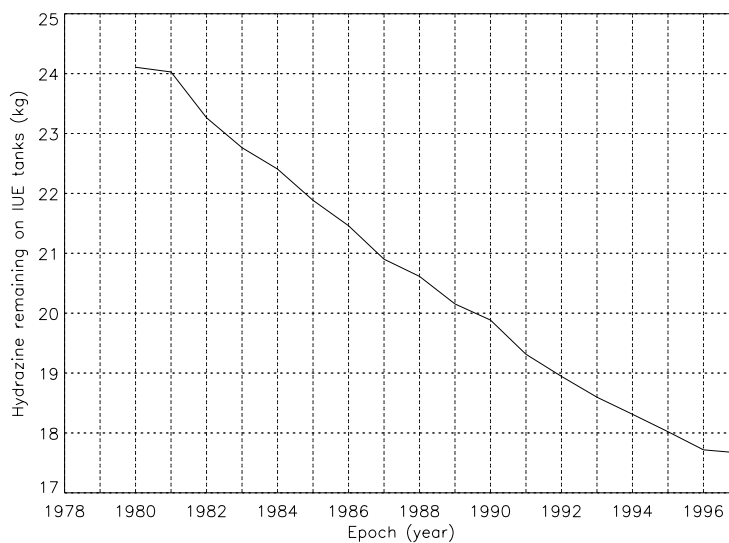
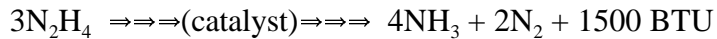


Figure 5-59. Hydrazine remaining on IUE tanks.

A jet can be fired in a continuous mode or a pulsed mode. In the continuous mode, the engine valve is activated and remains open until commanded to stop firing. The continuous mode was never used, except accidentally. In the pulsed mode, the engine valve is open only for 30 milliseconds, the hydrazine flows over the catalyst beds and this chemical reaction occurs:



These gases expand and are forced out of the nozzle producing the thrust.

The HAPS provides the spacecraft with the attitude torquing capability needed to perform the following functions:

- ▶ Nutation control. The spacecraft spun at a rate of approximately 60 rpm around its X axis after it was separated from the Delta third stage. Because it was an unfavourable moment of inertia axis, the spacecraft would develop an increasingly conical wobble, which, if unchecked, would cause it to enter into a flat spin around the transverse axis with a maximum moment of inertia. This conical wobble was monitored by the nutation sensor assembly (NSA). The NSA contains two redundant accelerometers which provide information for computing the nutation cone buildup. The spin axis nutation is controlled using either of the angled 5 pound thrust jets (jets 5 and 11). The firing of these jets was controlled by an onboard nutation control algorithm.
- ▶ Precession control. During the transfer orbit, the spacecraft was released from the Delta third stage with its ABM facing aft. After the separation, the spacecraft was precessed, or flipped, 180 degrees to facilitate the ABM burn. This precession maneuver maintained a constant solar array exposure. The maneuver was performed using the angled 5 pound thrusters (jet 5 and 11). During the precession maneuver, the NSA was disabled. After completion of the precession maneuver, the NSA was enabled to remove any nutation prior to the ABM burn and despin operations.
- ▶ Velocity correction to initially acquire the orbit station. After the ABM was commanded to ignite by ground command, the hydrazine provided the velocity change required to get on station. It was actually achieved with very little hydrazine consumption.
- ▶ Despin of the spacecraft. When the desired station was obtained, the spacecraft was despun in two phases to calibrate the HAPS thrusters and gain three-axis gyro rate control. The IUE was spun up to 2 to 5 degrees per second, and the solar arrays were deployed. After deployment, the IUE was rate damped to 0.25 degree per second. The solar acquisition phase was then initiated and the spacecraft was aligned with the sunline normal to the primary plane of the solar arrays.
- ▶ Spacecraft torquing to acquire proper Sun angle in the event of attitude loss. Rate + Position Hold mode was a backup attitude control configuration that is available in an emergency. An OBC program, Worker 19, used the information coming from the attitude sensors (initially gyros, in rate mode, only; under the 2 Gyro/FSS control mode, gyros, in rate mode, and FSS) to compute the jet torques.
- ▶ Velocity correction for east-west station keeping (Delta-V). The HTE's 2 & 8 were used to control the yaw axis and give the thrust to induce translational spacecraft motion while

LTE continued to provide pointing control in the pitch and roll axes. The three axes were controlled in a similar way to the Rate + Position Hold mode.

- ▶ Spacecraft torquing to unload reaction wheels. Firing a jet produces an external force upon the spacecraft. The gyros sense this force in the form of spacecraft rotations and send the information to the OBC. The jet firings produce both rotational and translational motion. The rotational motion, through hold/slew program's (worker 0) intervention, results in wheel velocities being changed. Worker 0 changes the wheel speeds in order to counteract the external force and keep IUE from moving. The translational motion was an ignored side-effect until a program was developed on October 2, 1989 to select the most favourable momentum wheel unload jet firing to counteract the westward drift of the spacecraft. This was done to reduce the frequency of the Delta-Vs.

The effectiveness of the HAPS in performing reaction wheel unloads depended largely on EV temperature, propellant tank pressure and catalyst bed temperature.

- ▶ High EV temperature were believed to cause the disassociation of the hydrazine within the fuel lines. Small pockets of disassociated or partially disassociated fuel produced low thrust when they move through the engine catalyst chambers.
- ▶ The system pressure affected how much fuel could be delivered to the engine per unit time. The continuing decrease in tank pressure due to fuel usage resulted in a decreased flow of hydrazine through a jet during a firing, decreasing the thrust of the jet.
- ▶ Catalyst beds are generally more efficient at higher temperatures. This was demonstrated in the low performance of the LTE which did not have chamber heaters, and in the locally high output of engines which had recently been fired and had higher than normal catbed temperatures.

Unload performance is measured by comparing the change in reaction wheel speed in each axis to the number of 30 millisecond engine firing pulses performed. The Δ RPM per pulse measurements for the single jet unloads are compared to the benchmark 1980 data and a composite percentage decrease is calculated. The figures 5-60, 5-61, 5-62, 5-63 and 5-64 demonstrate the trends in unload performance.

HAPS thermal design.

The mission requirements for thermal control throughout the HAPS unit were dictated by the freezing and vaporization points of the hydrazine fuel. The region was maintained above 5°C to prevent freezing, which would have both disrupted the fuel supply and damaged the control valve assemblies. The upper temperature limit on all HAPS component was initially set at 65°C but had to be raised to 85°C for all components except for two sensors, +ZLN and -ZLN, which had an upper limit of 90°C. This was done in a effort to reduce cycling of the catalyst bed heaters, after the HAPS heater group 1 failed due to excessive cycling.

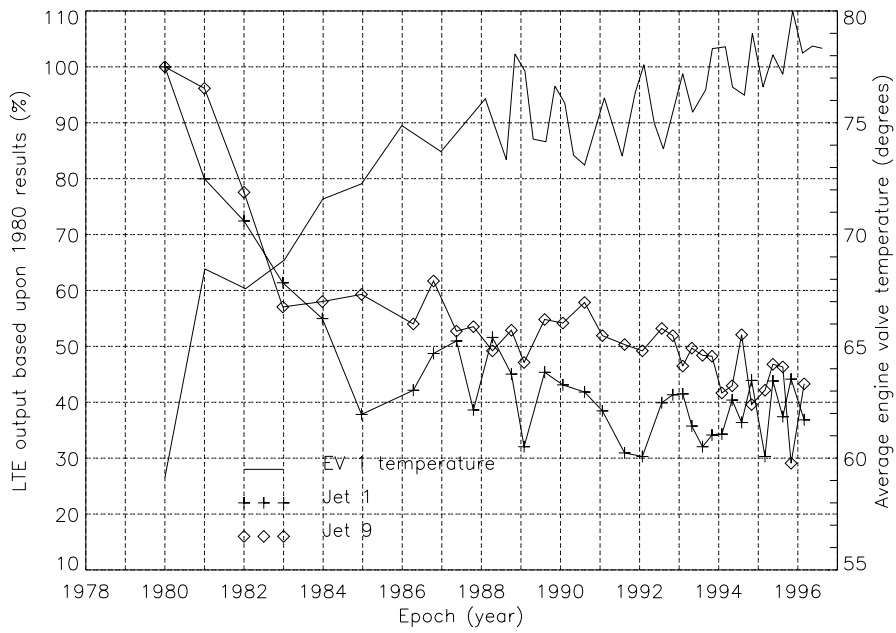


Figure 5-60. Comparison of LTE 1 & 9 output and associated EV 1 temperature.

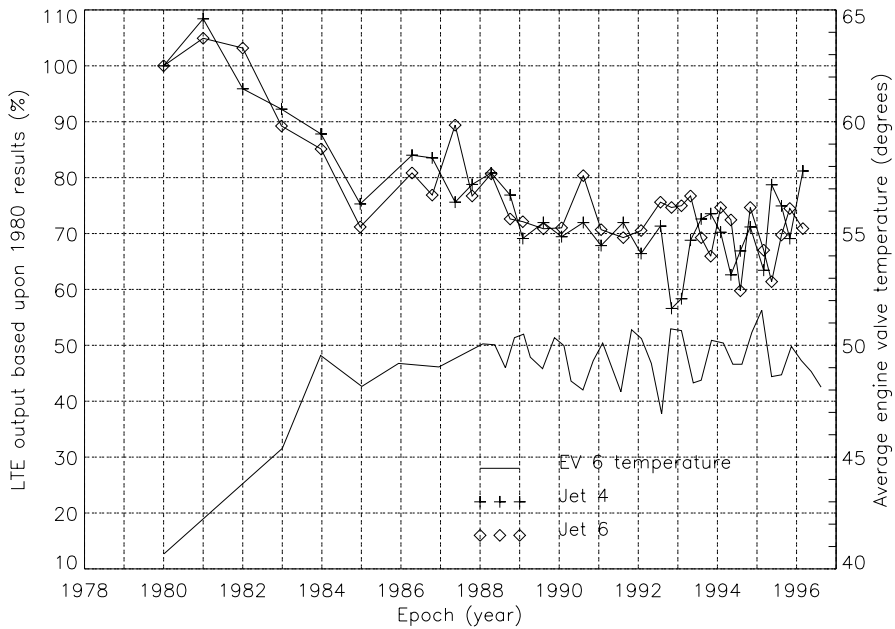


Figure 5-61. Comparison of LTE 4 & 6 output and associated EV 6 temperature.

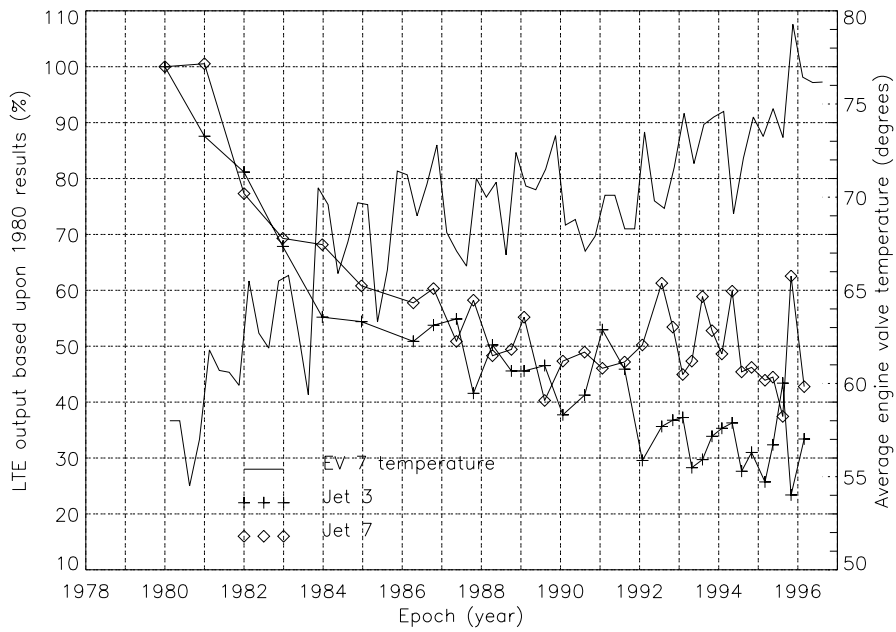


Figure 5-62. Comparison of LTE 3 & 7 output and associated EV 7 temperature.

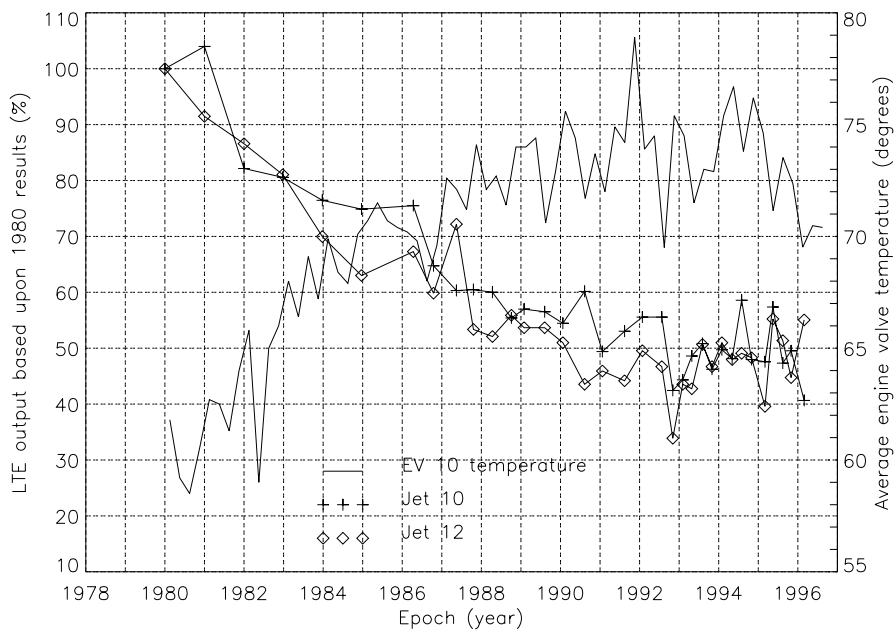


Figure 5-63. Comparison of LTE 10 & 12 output and associated EV 10 temperature.

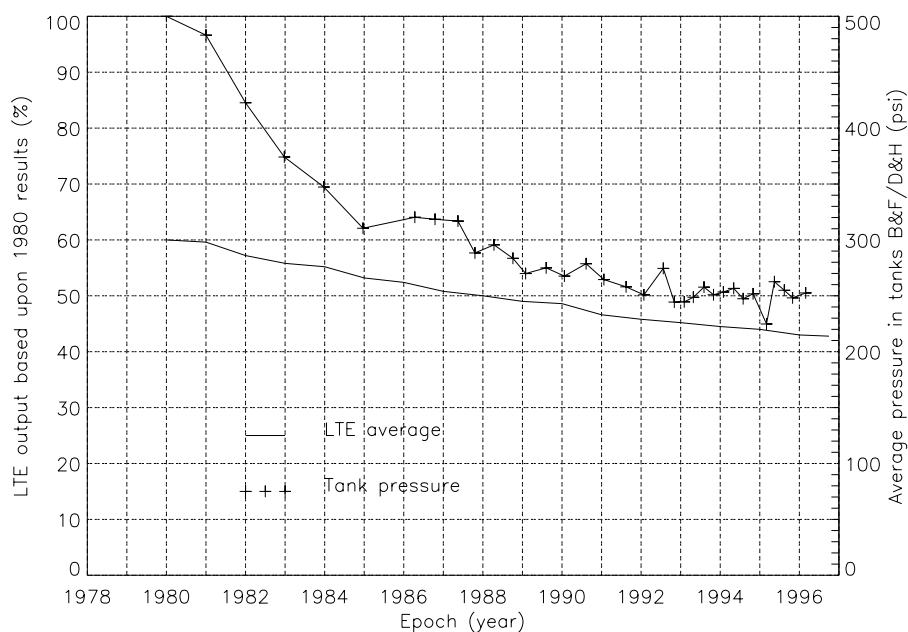


Figure 5-64. Comparison of LTE average output and hydrazine tank pressure.

Although there was a need for additional heater units, the primary thermal control was provided by solar energy. The following HAPS heater groups are present.

- Group 1. Primary chamber heaters LTE 1, 3, 4, 6, 7 and 9.
- Group 2. Backup heaters for group 1.
- Group 3. Backup heaters for group 7, plus primary heater on +Z hydrazine lines, hydrazine tanks B and H, and LTE 10 and 12 valves.
- Group 4. Primary heaters on +Y and -Y REM struts, +Y and -Y REM mount, and LTE 4 and 6 valves.
- Group 5. Backup heaters for group 4.
- Group 6. Primary heaters on HTE 5 and 11.
- Group 7. Primary heaters on -Z hydrazine line, hydrazine tanks C, D, F and G.

The IUE used only the low-thrust engine chamber heaters (HAPS heater group 1 and its backup, group 2). The other heaters were not needed during the mission because temperatures in the HAPS area remained higher than predicted.

5.5.9.1. HAPS heater group 1 failure.

On December 15, 1980 the heaters on jets 4 and 6 failed. They are wired in series with each other and in parallel with the other two pairs. The other heaters continued to function properly. A switch was made to heater group 2, backup for the low-thrust engines.

The cause of the failure was believed to be excessive cycling. To guard against this type of failure again, the decision was made to raise the red-line limits of the HAPS to 85°, and only turn off the heater group when that limit was reached. This option was chosen at the recommendation of the HAPS designers, who preferred a hot HAPS rather than firing cold jets. The problem with an 85° limit on the HAPS was a possibility of hydrazine decomposing and gas bubbles forming near the engine valves. These gas bubbles would not cause any harm but would show up as weak firings or give the appearance of a missing pulse in a unload. Operationally, it was a simple matter to just uplink commands for more pulses, so this reduced thrust was a minimum problem.

5.5.9.2. N₂H₄ venting.

On September 30, 1996 the N₂H₄ venting procedure was performed and was the start of the final shut down operations. The need to vent the remaining N₂H₄ was based on the assumption that eventually after being left unattended, the HAPS system components would freeze and thaw. This action would lead to a structural failure of the system venting N₂H₄, which could be catastrophic to any ill-fated satellite in the vicinity of IUE. The venting process decomposed the N₂H₄ eliminating this possible event.

The venting procedure was named the roll spin venting method. In this method of N₂H₄ venting, the spacecraft was maneuvered to a specified attitude, which was selected to give a planned change to the orbit based on the expected Delta-V that resulted from the venting process. Once at the desired target, all the non-essential pieces of equipment were powered off. The pitch and yaw reaction wheels were dumped as close to zero as possible, while the roll wheel was dumped close to the saturation limit (around 1460 rpm) to cause +Roll rotation of spacecraft. Then, the reaction wheels were disabled. There was no control on the spacecraft pointing attitude at this time, so IUE began to spin.

The valve 2 was open at approximately 15:10 UT. The N₂H₄ venting was achieved in approximately two hours while several jets were firing in continuous mode. The figures 5-65 and 5-66 show the tank temperatures and pressures during the venting (the B&F tank pressure is not present due to its sensor pressure failure).

The LTE's used to spin up the spacecraft were selected so that most of the non-Roll axis momentum was cancelled, although the spin was not purely about the Roll axis since all of the LTE's have a Roll component as well as a component in either the Pitch and Yaw axis. While the jets were fired, high temperatures were reached (around 170°C). The figure 5-67 shows the LTE's and HTE's used. In the last minutes, the HTEs were fired due to the slow venting achieved with the LTE's.

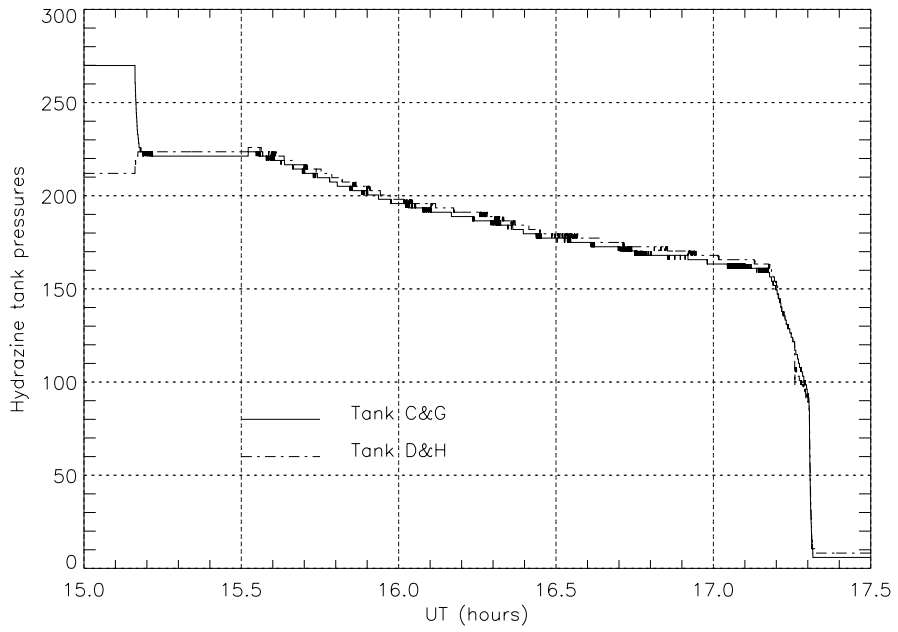


Figure 5-65. Tank pressures during the N_2H_4 venting.

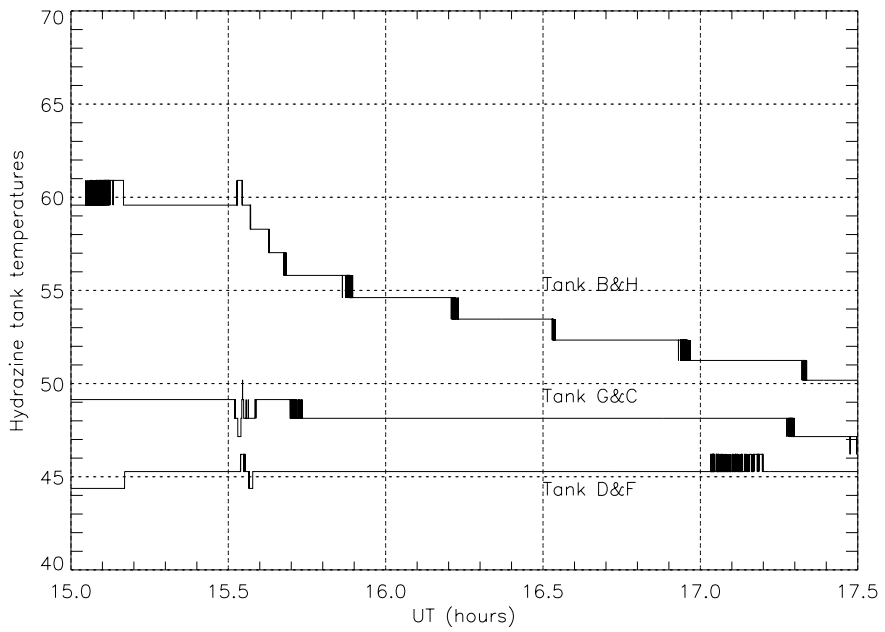


Figure 5-66. Tank temperatures during the N_2H_4 venting.

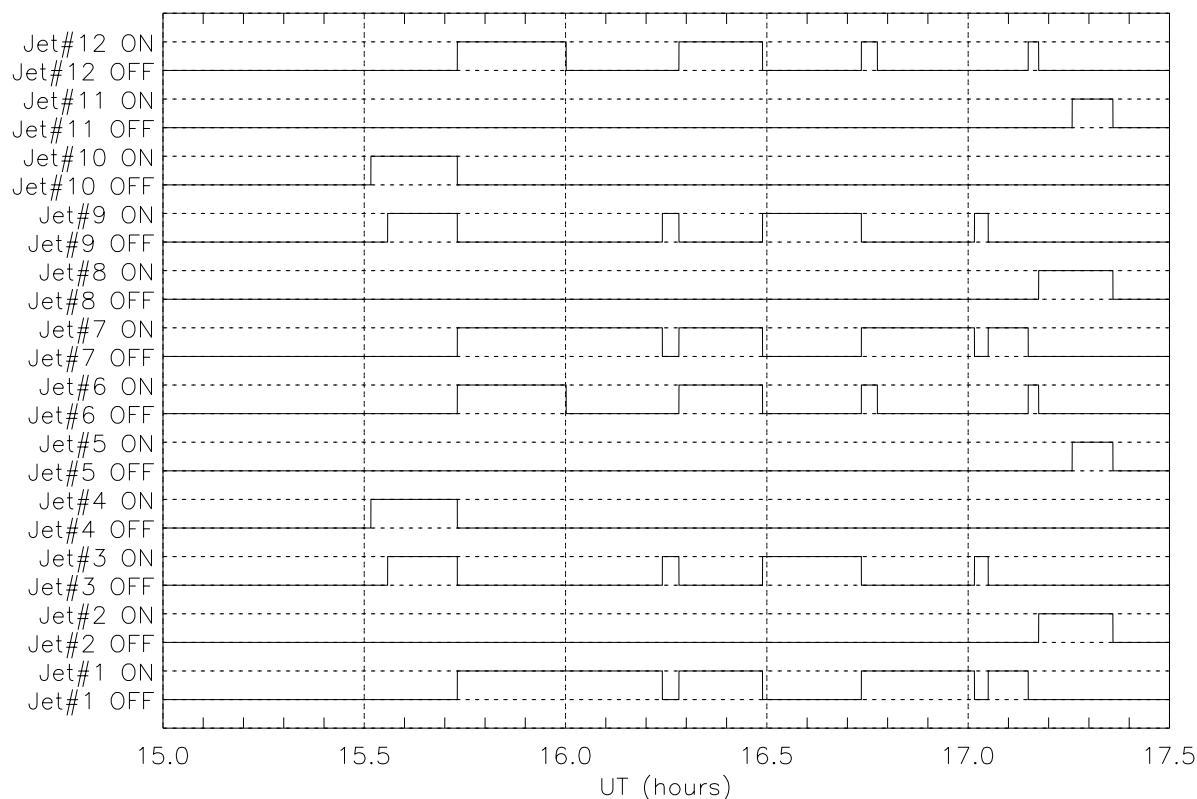


Figure 5-67. Jets fired during the N_2H_4 venting.

5.5.10. Control Electronics Assembly.

The Control Electronics Assembly (CEA) which provides the interface between the sensors and the actuators performs the following functions: provides certain hardwired logic functions (primarily through the launch phase commencing at Delta separation and ending after Sun acquisition in elliptical synchronous orbit), provides power switching internal and external to the unit, decodes digital command words from the OBC, generates analog signals for inertial wheel driving, provides high-level signals for energizing hydrazine thrusters and provides telemetry conditioning for the various telemetry sensors in the HAPS.

The unit consists of eight cards with functions as defined below.

- **Card 1. Precession/Nutation Card.**

This card provides the digital logic for spin sectoring, precession commands, active nutation control and engine mode selection. The spin sectoring portion receives a sun-centered pulse from the PAS and an input from the spacecraft clock. With this information available, the spin period is divided into 128 parts. The current sector status (position) is maintained and updated throughout each spin cycle. This logic information on the spin

status is interfaced with both the precession command logic and active nutation control logic. In the precession logic the current sector status is compared with a ground command consisting of three parts: sector ID to start firing a precession thruster, sector ID to stop firing a precession thruster and the number of consecutive spin cycles during which the precession jet will be fired.

- **Card 2. Relay Card.**

This module contains a bank of latch relays and relay drivers to enable power switching to all cards within the control electronics assembly and wheel driver assembly. The effect of switching between the buses is not only to ensure power by being able to select between redundant buses, but to remove power from unneeded functions by switching them to the standby bus.

- **Card 3. Digital-to-Analog Converter and Wheel Commands.**

These are redundant cards that develop the analog signals used by the wheel drivers. Reaction wheel commands are serially gated into this card from either Command Decoder and converted to analog voltages for the pitch, yaw, roll and redundant wheel drivers.

- **Card 4. Engine Valve Command Logic.**

These are redundant cards that provide low-level signals used by the engine valve drivers to activate the hydrazine system. Inputs to the cards are through the spacecraft command system, DMU, compensation/mixing card and the precession/nutation card.

- **Card 5. Compensation/Mixing Card.**

This card receives analog sun sensor information and rate information and combines them to form logic levels to drive the low level thrusters during despin and sun acquisition. In addition, this card drives the reaction wheels during the sun hold mode of operation (SUNBATH mode) which serves as a backup in the event of an OBC hangup preventing the normal digital control algorithm from being processed. In this mode, the card receives position from the set of six coarse sun sensors distributed about the IUE spacecraft. These signals are combined and the analog error signals are used to drive the reaction wheels.

- **Card 6. HAPS Telemetry Conditioning Card.**

The functions of this card are to condition the signals to and/or from the various temperature and pressure sensors in the HAPS and monitor and indicate the positions of various latch valves between tanks and manifolds and jet valves. This card is powered by the redundant power supplies in the wheel driver assembly.

- **Card 7. Engine/Valve Driver Cards 1 and 2.**

These redundant cards serve as the power stage to drive the hydrazine system's engine solenoids and transfer valve solenoids. The output from each of the redundant cards are logically OR'ed together via isolation diodes to drive the common solenoids.